Solid-State Electronics 69 (2012) 50–54

Contents lists available at SciVerse ScienceDirect

Solid-State Electronics

journal homepage: www.elsevier.com/locate/sse

Hybrid solar cells with an inverted structure: Nanodots incorporated ternary system

Honghong Fu [a], Mijung Choi [b], Weiling Luan [a,*], Yong-Sang Kim [b,*], Shan-Tung Tu [a]

[a] Key Laboratory of Pressure Systems and Safety, Ministry of Education, School of Mechanical and Power Engineering, East China University of Science and Technology, Shanghai 200237, China
[b] Department of Nano Science and Engineering, Myongji University, Gyeonggi 449-728, Republic of Korea

ARTICLE INFO

Article history:
Received 22 May 2011
Received in revised form 1 November 2011
Accepted 21 December 2011
Available online 12 January 2012

The review of this paper was arranged by Y. Kuk

Keywords:
CdSe nanodots
Hybrid solar cell
Ternary system
Inverted structure
Stability

ABSTRACT

Ternary system hybrid solar cells that are composed of CdSe nanodots, poly (3-hexylthiophene) (P3HT) and phenyl-C_{61}-butyric acid methyl ester (PCBM) with an inverted structure were investigated. The incorporation of 10 wt% CdSe nanodots showed increased power conversion efficiency (PCE) of 3.05% compared with that of a binary system with P3HT and PCBM, which is comparable with the best reported efficiency of nanocrystal based solar cells. The photophysical energy level of inverted structure and electrochemical, optical properties and microscopy images of the ternary systems were systematically investigated to elucidate the mechanism. The obtained hybrid solar cell showed enhanced stability through exposure in ambient condition without any encapsulation.

1. Introduction

Organic hybrid solar cells based on semiconductor nanocrystals are among the most promising alternatives to traditional silicon solar cells. In a hybrid solar cell system, both semiconductor nanocrystals and polymers act as sunlight absorbers and exciton generators. The polymer works as electron donors, while the semiconductor nanocrystal works as acceptors. Moreover, the electron transportation in nanocrystals is much faster than that in polymers. As the absorption wavelength of the nanocrystals can be tuned according to size, composition and shape [1], it can be well matched to the solar radiation spectrum. Hence, solar cells incorporated with nanocrystals show great potentials in achieving better efficiency compared with silicon solar cells [2].

CdSe is one of the most popular nanocrystals used in hybrid solar cells. In 1996, Greenham [3] fabricated the first hybrid solar cell with CdSe nanodots, which showed a PCE of 0.01%. Then Huynh [4] fabricated devices to compare the effect of CdSe with different morphologies. As CdSe nanorods provide enhanced charge transportation properties in comparison with CdSe nanodots, an improved PCE of 1.7% was observed. Further elevated efficiencies were obtained by incorporating other shapes of CdSe, such as nanowires, tetrapods [5,6] and hyperbranches [7]. Recently, Dayal et al. [8] reported a new PCE record of 3.2% with CdSe tetrapods and a low band-gap polymer. However, because of the inefficient electron transport caused by multiple hopping events among the nanodots, the device efficiencies with nanodots are several times lower than those with nanorods or tetrapods. Except for the PCE value of 2% reported by Zhou et al. [9], most of the other efficiencies with CdSe nanodots are usually less than 1% [10,11].

Up to now, researches on nanocrystal polymer hybrid solar cells have been mainly based on binary systems. Studies on ternary systems which are composed of polymers, PCBM and nanocrystals are rarely reported [12,13]. Chin and co-workers [14] incorporated Au nanocrystals in a P3HT and PCBM system, and an increased short circuit current density (J_{sc}) was obtained. Nogueira [15] investigated ternary systems with mixtures of PFT, CdSe and PCBM. By optimizing the ratio of CdSe to PCBM and particle size, higher photocurrents and PCE were obtained.

The conventional organic solar cell structure includes a transparent indium tin oxide (ITO) layer for hole collecting, a poly(3,4-ethylenedioxythiophene):poly(sty-renesulfonate) (PEDOT:PSS) layer for hole transportation, a bulk heterojunction active layer, and a metal electrode layer for electron collecting. However, the interface between the acidic anodic buffer layer PEDOT: PSS and a common

* Corresponding authors. Addresses: School of Mechanical and Power Engineering, East China University of Science and Technology, No. 130 Meilong Road, Shanghai 200237, China. Tel./fax: +86 21 6425 3513 (W. Luan), Department of Electrical Engineering/Nano Science and Engineering, Myongji University, 38-2 Nam-dong Yongin, Gyeonggi 449-728, Republic of Korea. Tel.: +82 31 330 6365; fax: +82 31 321 0271 (Y.-S. Kim).

E-mail addresses: luan@ecust.edu.cn (W. Luan), kys@mju.ac.kr (Y.-S. Kim).

0038-1101/$ - see front matter © 2011 Elsevier Ltd. All rights reserved.
doi:10.1016/j.sse.2011.12.009

transparent electrode such as ITO has been proven unstable in air, especially under humid conditions [16]. The inverted structure with TiO_2 as an electron selective layer and with PEDOT: PSS as a hole selective layer is proven to be of high stability and PCE [17].

In this paper, ternary system hybrid solar cells consisting of CdSe nanodots, P3HT and PCBM with an inverted structure were fabricated. The devices were fully characterized and the effect of the incorporation of CdSe nanodots was discussed. The stability of the CdSe nanodots added solar cells were also investigated.

2. Experimental

2.1. Materials and CdSe nanodot preparation

PCBM and regioregular P3HT were purchased from Sigma Aldrich, and were used as received. CdSe nanodots were synthesized following the protocol described in literatures [18,19]. The obtained CdSe nanodots were dispersed in chloroform and were washed several times with excess of acetone. To achieve an efficient charge transfer between the polymer and CdSe, surface modification was conducted by exchanging the ligand of CdSe with pyridine. After the ligand exchange and purification, the final CdSe nanodots were dried with a flow of nitrogen gas.

2.2. Active layer solution preparation

The hybrid nanocomposite solution was prepared by dissolving 60 mg P3HT and 60 mg PCBM in 4 ml chlorobenzene to achieve a concentration of 30 mg/ml. Subsequently, 6 mg CdSe nanodots were added to the solution making a 10% weight ratio to P3HT and PCBM. The solution was stirred for 24 h before device fabrication.

2.3. Cyclic voltammetry of CdSe nanodots

The HOMO and LUMO values of CdSe nanodots were obtained via cyclic voltammetry (CV). CV curves were recorded using an electrochemical workstation (CH instrument, USA, model 800B), using a glassy carbon disk as the working electrode, a Pt wire as the counter electrode and Ag/AgCl as the reference electrode. Afterward, 0.1 M tetrabutylammonium hexafluorophosphate ($TBAPF_6$), dissolved in acetonitrile was used as the supporting electrolyte. Then, 0.01 M purified CdSe nanodots were dispersed in chloroform to get a uniform solution and then coated on the surface of the working electrode, which had already been cleaned, polished and dried. Cyclic voltammograms were recorded at a scan rate of 0.02 V/s.

2.4. Device fabrication

The schematic graph of the solar cell is shown in Fig. 1. Glass substrates pre-coated with fluorine tin oxide (FTO) (with a size of 2 cm × 2 cm and a sheet resistance of 15 Ω/square) were cleaned in ultrasonic baths of acetone and isopropanol for 30 min respectively, and were dried with a nitrogen flow. The TiO_2 sol–gel solution was prepared by mixing titanium (IV) ethoxide, HCl and isopropyl alcohol. The TiO_2 solution was spin-coated on the FTO substrate and then sintered at 500 °C for 2 h in an ambient condition. The thickness of TiO_2 was 140 nm as measured by a surface profiler (alpha-step). The active layer composed of P3HT, PCBM and CdSe was spin-coated on the TiO_2 layer. Approximately 40 nm PEDOT:PSS layer was spin-coated on the active layer and then annealed at 150 °C for 10 min on a hot plate. Finally, Ag electrode with the thickness of 100 nm was thermally evaporated with active device area of 0.1 cm^2.

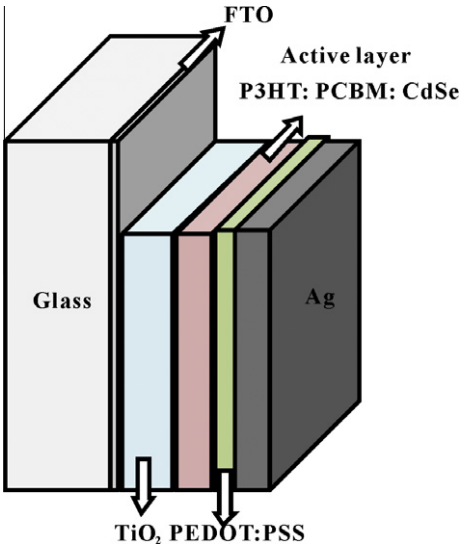

Fig. 1. Schematic diagram of the ternary system solar cell.

2.5. Characterization

The hybrid solar cells were characterized in air without any encapsulation. The current density versus voltage (*J–V*) characteristics were measured by a *J–V* curve tracer (Eko MP-160) with a solar simulator (Yamashita denso) under AM 1.5G (100 mW/cm^2) irradiation intensity. UV/visible spectrophotometer (Shimadzu UV-1601) was used for the absorption spectra measurement of the active layers. The UV/vis absorption spectra of CdSe nanodots were measured using Cary 50 UV–visible spectrometer (Varian, USA). The surface morphology of the active layer was measured by field-emission transmission electron microscope (FE-TEM, JEM-2100F, JEOL). The ITO/glass substrates coated with PEDOT:PSS and P3HT:PCBM:CdSe films were immersed in deionized water for a few minutes to dissolve the PEDOT:PSS. A carbon-coated copper grid was then used to pick up the active layer films floating on the water surface. The hybrid films were dried naturally in air and observed with TEM for characterization.

3. Results and discussions

3.1. Optical properties of CdSe nanodots and active films

Fig. 2 displays the absorption characteristic of the synthesized CdSe nanodots. Two distinct absorption peaks at 565 nm and 460 nm were observed in the UV-vis absorption spectrum. From the absorption spectrum, we can estimate the diameter of the

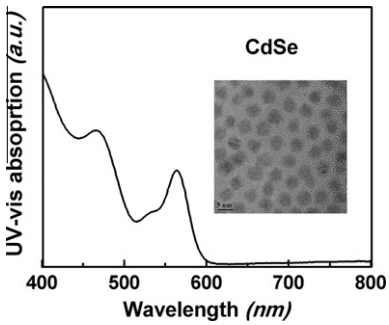

Fig. 2. UV–vis absorption spectrum of CdSe nanodots (inset: HRTEM image of CdSe).

nanodots using the equation proposed by Yu et al.[20]. The calculated average size of the CdSe nanodots is around 3.5 nm, which is consistent with the value obtained from the HRTEM image. Relatively narrow HWHM (half width at half maximum) from the absorption spectrum indicated that the synthesized CdSe nanodots were monodispersed.

$$D_a = (1.6122 \times 10^{-9})\lambda_{max}^4 - (2.6575 \times 10^{-6})\lambda_{max}^3 + (1.6242 \times 10^{-3})\lambda_{max}^2 - (0.4277)\lambda_{max} + 41.57 \quad (1)$$

here, Da is the diameter size of the nanoparticle; λ_{max} is the wavelength of the first exciton peak.

In Fig. 3, UV–vis absorption spectra of active layer films consisting of P3HT, PCBM (P3HT:PCBM) and P3HT, PCBM and CdSe (P3HT:PCBM:CdSe) were compared. Two peaks were found in the absorption profile of binary system (P3HT:PCBM). The 330 nm peak corresponds to the absorption of PCBM, while the 490 nm corresponds to P3HT. After incorporation of CdSe nanodots, an obvious enhancement of absorption intensity and red shift of absorption peak were observed. The area under the absorption profile indicates the light-harvesting ability of the active film. An increase in ~10% absorption area was calculated for ternary system, which means more photons were harvested. Besides, the main solar radiation spans the region from the visible light to the near-infrared zone (just as the inset spectrum in Fig. 3), and the radiation intensity show a parabola profile with the wavelength. The highest radiation intensity was obtained nearby 700 nm. The red shift of the absorption profile expands the match to solar radiation spectrum. Hence, more photons were utilized and more charges were generated.

3.2. The effect of the CdSe nanodots on the hybrid solar cell

In Fig. 4, the *J–V* characteristics of solar cells fabricated with the ternary system (P3HT:PCBM:CdSe) and the binary system (P3HT:PCBM) were compared. All the devices were fabricated with the same active layer thickness of around 80 nm (measured by alpha-step). From the *J–V* characteristics, an obvious performance enhancement was observed in the ternary system. With the incorporation of 10% CdSe, the J_{sc}, open circuit voltage (V_{oc}), fill factor (FF) and PCE were all improved. The detailed values of the parameters are listed in Table 1.

The increase of J_{sc} from 7.51 mA/cm^2 to 8.15 mA/cm^2 was attributed to the improvement of light harvesting capability of CdSe in solar cells, which has already been stated before. Besides, the electron transportation is applied to validate the J_{sc} enhancement. The CdSe nanodots were synthesized with oleic acid (OA),

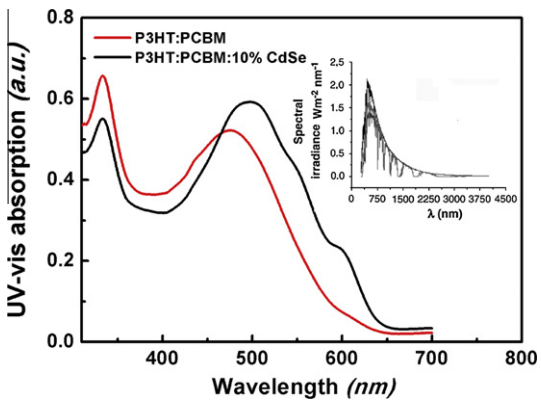

Fig. 3. UV–vis absorption spectra of active layer films of P3HT:PCBM:10 wt.% CdSe (inset: the standard air mass (AM)1.5 global solar spectrum).

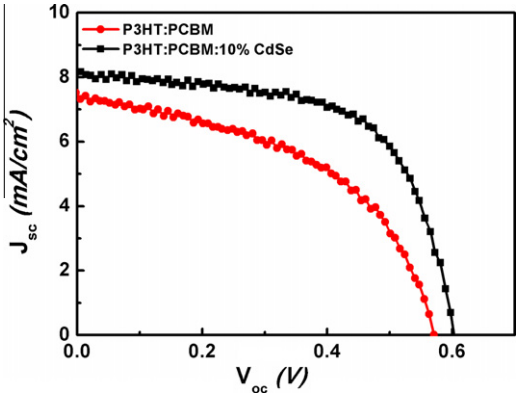

Fig. 4. *J–V* characteristics of fabricated solar cells with the ternary system (P3HT:PCBM:CdSe) and the binary system (P3HT:PCBM). (Solar cells illuminated at 100 mW/cm^2; the active area is 0.1 cm^2.)

Table 1
Photovoltaic parameters obtained for solar cells with binary and ternary systems.

	Ternary system (P3HT:PCBM:10% CdSe)	Binary system (P3HT:PCBM)
J_{sc} (mA/cnf)	8.15	7.51
V_{oc} (V)	0.60	0.57
FF	0.62	0.48
PCE (%)	3.05	2.06

and the OA is long chain ligand, it always became the recombination centre of electrons. The ligand exchanging with short chain pyridine helps to achieve efficient charge transfer between the polymer and CdSe by reducing the recombination. And after ligand exchanged, the CdSe nanodots aggregated. The surface morphology of the active film of P3HT:PCBM:CdSe (Fig. 5) showed that the CdSe nanodots were randomly dispersed in the film. When the active film was deposited, CdSe nanodots aggregated to form clusters larger than 50 nm because of the weak binding energy of pyridine around the surface of CdSe. The nanodot aggregation facilitates the electron transportation, according to the potential for the formation of efficient percolation pathway in the photoactive film, resulting in increased J_{sc} without modification of shape.

The V_{oc} of the ternary system based solar cell was increased from 0.57 V to 0.60 V after the addition of CdSe nanodots, and the increase of V_{oc} was most probably attributed to the enhancement of the charge separation, which can be disclosed by the energy levels of the solar cells (as shown in Fig. 6). The HOMO and LUMO levels of CdSe nanoparticles were measured via CV and were calculated with the following equations [21]:

$$E_{HOMO} = -(E'_{OX} + 4.71)\text{eV} \quad (2)$$

$$E_{LUMO} = -(E'_{red} + 4.71)\text{eV} \quad (3)$$

$$Eg_{CV} = E_{LUMO} - E_{HOMO}\text{eV} \quad (4)$$

where, E'_{ox} is the potential of the onset oxidation peak, E'_{red} is the potential of the onset reduction peak and Eg_{cv} is the band gap calculated from CV.

E'_{ox} and E'_{red} were obtained from the CV curves of CdSe, and E_{LUMO} was calculated as -3.7 eV, while E_{HOMO} was −5.9 eV. The Eg_{CV} was 2.2 eV, which is consistent with the band gap obtained from the UV–vis spectrum (2.1 eV) with a deviation of around 4.76%.

Upon incidence of the irradiation, both polymer and CdSe nanodots absorb photons and generate excitons. The excitons separate at the donor–acceptor interfaces. For electrons, they can be

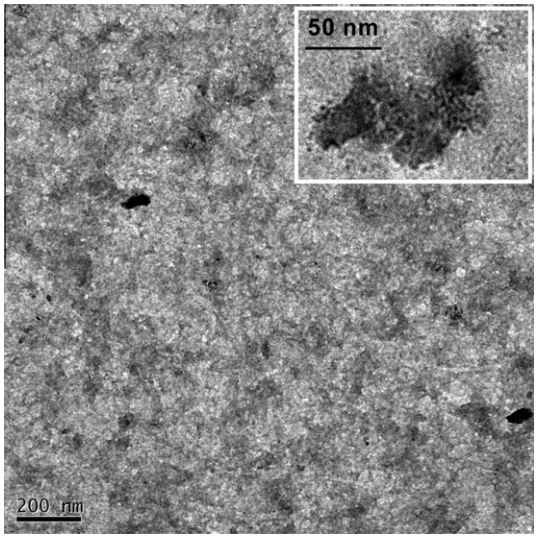

Fig. 5. TEM image obtained with a ternary system film (P3HT:PCBM:10% CdSe).

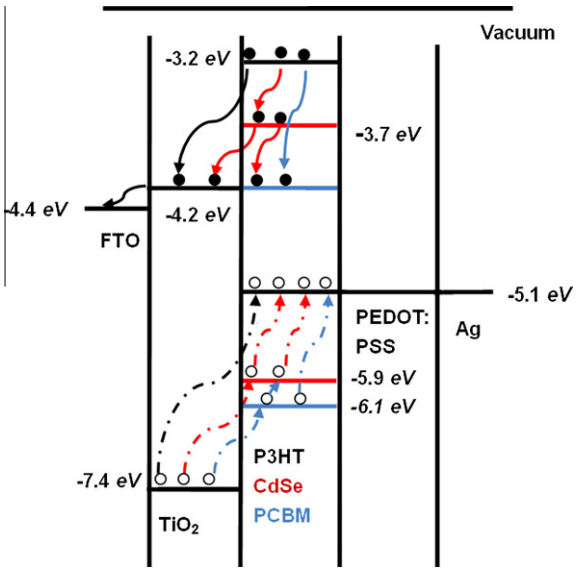

Fig. 6. Schematic diagram of the energy levels of the ternary system solar cells. (black circles represent the electrons, while the white ones represent the holes, the black curve with arrow represents the exciton transfers via P3HT, the red one represents the exciton transfers via CdSe, and blue one represents the exciton transfers via PCBM). (For interpretation of the references to colour in this figure legend, the reader is referred to the web version of this article.)

transferred from P3HT to TiO_2 (just as the black curve with arrow in Fig. 6). The second route for electrons is transferred from P3HT to PCBM (just as the blue curve with arrow in Fig. 6), another route is from P3HT to CdSe (just as the red curve with arrow in Fig. 6). However, with the absence of CdSe nanodots, this extra donor-acceptor interface (P3HT:CdSe) was not exited. And as the LUMO level of CdSe is calculated to be −3.7 eV, while it is −4.2 eV for PCBM, so electrons can also be transferred from CdSe to PCBM. Then the electrons can be finally collected by FTO, because the LUMO values of both PCBM and TiO_2 are −4.2 eV, while the work function of FTO is −4.4 eV. With the presence of CdSe, extra electron transport route was occurred. The hole transportation is accomplished inversely. It is believed that P3HT:PCBM, P3HT:CdSe and CdSe:PCBM interfaces result in more efficient charge separations and collections, resulting in a larger V_{oc}.

The FF of the solar cell device with CdSe nanodots was 0.62 and the PCE was 3.05%. And the PCE of 3.05% was the highest efficiency reported ever since the incorporation of CdSe nanodots.

This promising performance was attributed due to the following mechanisms: the incorporation of CdSe increased the sunlight harvesting, more photons were absorbed and more charges were generated. Besides, CdSe is used as the electron transport material in this ternary system hybrid solar cell, the intrinsic mobility of inorganic semiconductor CdSe nanodot is higher than polymer materials. For many conjugated polymers, electron mobility is extremely low due to the presence of ubiquitous electron traps such as oxygen. Meanwhile, after pyridine exchange, the CdSe nanodots aggregation occurred when the active film was deposited, which facilitated the electron transport according to the potential for the formation of efficient percolation pathway in the photoactive film, resulting in a larger J_{sc}. Then, the inverted structure with TiO_2 as the electron collection layer offered extra donor–acceptor interfaces after the incorporation of the CdSe nanodots, resulting in multiple electron transport routes. Furthermore, because of the appropriate LUMO value of TiO_2, the effective electrons were injected into TiO_2 easily while the holes were blocked.

3.3. Stability of the device

One of the disadvantages of organic solar cells is the low stability. The reported efficiency of a pure organic solar cell based on P3HT and PCBM can be as high as 5%. However, the relatively low stability blocks its development. In this paper, the stability of the fabricated solar cells was also studied.

All the devices were fabricated as stated above and stored in ambient air without any encapsulation for 21 days, and then the devices were periodically measured. As can be seen from Fig. 7, J_{sc} gradually decreased from 8.15 mA/cm^2 to 6.82 mA/cm^2, while

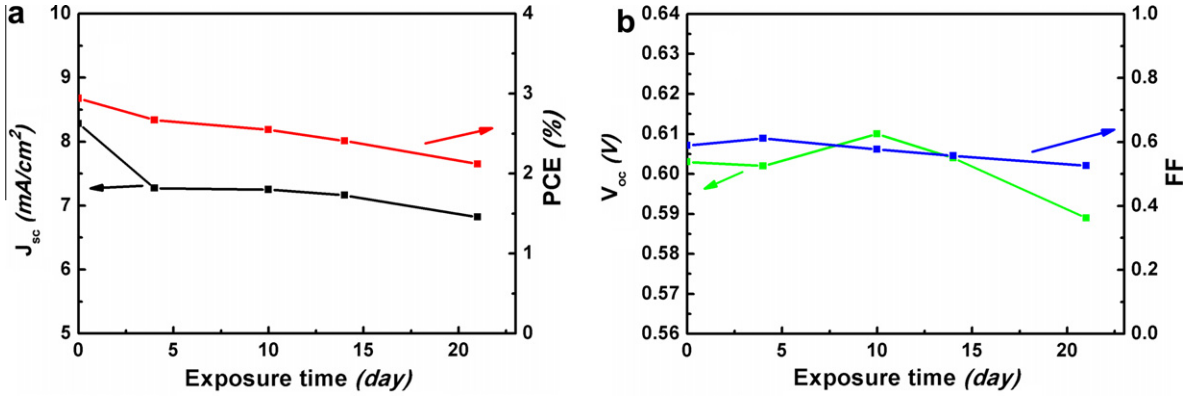

Fig. 7. Stability of ternary system solar cells with an inverted structure.

PCE decreased from 3.05% to 2.15% (Fig. 7a), and V_{oc} kept almost constant during the measurement period (Fig. 7 b). As a result, over 70% of its original efficiency was remained, which shows great potential for future applications.

4. Conclusions

Inverted structure hybrid solar cells that were based on ternary system of P3HT, PCBM and CdSe nanodots were investigated. The solar cells that incorporated CdSe nanodots showed enhanced performance as compared with the binary system of P3HT and PCBM. An efficiency of 3.05% was achieved, which is comparable with the record efficiency of shape-tailored CdSe based solar cells. Furthermore, the ternary system solar cell with an inverted structure was proven to be of a high stability, a quite stable performance was observed, 70% of its initial efficiency remained after 21 days of exposure in air.

Acknowledgements

We gratefully acknowledge financial support from the Fundamental Research Funds for the Central Universities (WJ0913001), The National Nature Science Fundation of China (51172072), the Focus of Scientific and Technological Research Projects (109063) and the State Key Laboratory of Chemical Engineering at ECUST (SKL-ChE-08C09). Honghong Fu is also grateful to the China Scholarship Council for financial support.

References

[1] Murray CB, Kagan CR, Bawendi MG. Synthesis and characterization of monodisperse nanocrystals and close packed nanocrystal assemblies. Annu Rev Mater Sci 2000;30:545–610.
[2] Nozik AJ. Exciton multiplication and relaxation dynamics in quantum dots: applications to ultrahigh-efficiency solar photon conversion. Inorg Chem 2005;44:6893–9.
[3] Greenham NC, Peng X, Alivisatos AP. Charge separation and transport in conjugated-polymer/semiconductor nanocrystal composites studied by photoluminescence quenching and photoconductivity. Phys Rev B 1996;54:17628–37.
[4] Huynh WU, Dittmer JJ, Alivisatos AP. Hybrid nanorod-polymer solar cells. Science 2002;295:2425–7.
[5] Zhou Y, Li Y, Zhong H, Hou J, Ding Y, Yang C, et al. Hybrid nanocrystal/polymer solar cells based on tetrapod-shaped $CdSe_xTe_{1-x}$ nanocrystals. Nanotechnology 2006;17:4041–7.
[6] Sun B, Marx E, Greenham NC. Photovoltaic devices using blends of branched CdSe nanoparticles and conjugated polymers. Nano Lett. 2003;3:961–3.
[7] Gur I, Fromer NA, Chen CP, Kanaras AG, Alivisatos AP. Hybrid solar cells with prescribed nanoscale morphologies based on hyper branched semiconductor nanocrystals. Nano Lett 2007;7:409–14.
[8] Dayal S, Kopidakis N, Olson DC, Ginley DS, Rumbles G. Photovoltaic devices with a low band gap polymer and CdSe nanostructures exceeding 3% efficiency. Nano Lett 2010;10:242–93.
[9] Zhou Y, Riehle FS, Yuan Y, Schleiermacher HF, Niggemann M, Urban GA, et al. Improved efficiency of hybrid solar cells based on non-ligand-exchanged CdSe quantum dots and poly(3-hexylthiophene). Appl Phys Lett 2010;96:013304.
[10] Choi SH, Sung H, Park IK, Yum JH, Kim SS, Lee S, et al. Synthesis of size-controlled CdSe quantum dots and characterization of CdSe-conjugated polymer blends for hybrid solar cells. J Photochem Photobiol A 2006;179:135–41.
[11] Tang AW, Teng F, Jui H, Gao Y, Hou Y, Liang C, et al. Investigation on photoconductive properties of MEH-PPV/CdSe-nanocrystal nanocomposites. Mater Lett 2007;61:2178–81.
[12] Naidu BVK, Park JS, Kim SC, Park SM, Lee EJ, Yoon KJ, et al. Novel hybrid polymer photovoltaics made by generating silver nanoparticles in polymer:fullerene bulk-heterojunction structures. Sol Energy Mat Sol C 2008;92:397–401.
[13] Morfa AJ, Rowlen KL, Reilly TH, Romero MJ, Van de Lagemaat J. Plasmon-enhanced solar energy conversion in organic bulk heterojunction photovoltaics. Appl Phys Lett 2008;92:013504.
[14] Park M, Chin BD, Yu JW, Chun MS, Han SH. Enhanced photocurrent and efficiency of poly(3-hexylthiophene)/fullerene photovoltaic devices by the incorporation of gold nanoparticles. J Ind Eng Chem 2008;114:382–6.
[15] Freitas JN, Grova IR, Akcelrud LC, Akcelrud LC, Arici E, Sariciftci NS, et al. The effects of CdSe incorporation into bulk heterojunction solar cells. J Mater Chem 2010;20:4845–53.
[16] Jørgense M, Norman K, Krebs FC. Stability/degradation of polymer solar cells. Sol Energ Mate Sol C 2008;92:686–714.
[17] Baek WH, Yoon TS, Lee HH, Yun CM, Kim YS. Hybrid inverted bulk heterojunction solar cells with nanoimprinted TiO2 nanopores. Sol Energy Mater Sol C 2009;93:1587–91.
[18] Yang H, Luan W, Tu ST, Wang ZM. High-temperature synthesis CdSe nanocrystals in a serpentine microchannel: wide size tuability achieved under short residence time. Cryst Growth Des 2009;9:1569–75.
[19] Yang H, Luan W, Tu ST, Wang ZM. Synthesis of nanocrystals via microreaction with temperature gradient: towards separation of nucleation and growth. Lab Chip 2008;8:451–5.
[20] Yu WW, Qu LH, Guo WZ, Peng X. Experimental determination of the extinction coefficient of CdTe, CdSe, and CdS nanocrystals. Chem Mater 2003;15:2854–60.
[21] Sun Q, Wang H, Yang C, Li Y. Synthesis and electroluminescence of novel copolymers containing crown ether spacers. J Mater Chem 2003;13:800–6.